Plasma Chemistry and Plasma Processing, Vol. 9, No. 1, 1989

Behavior of Particulates in Thermal Plasma Flows

Y. P. Chyou[1] and E. Pfender[1]

Received February 18, 1988; revised April 28, 1988

Injection of particulate matter into a thermal plasma represents one of the approaches used in thermal plasma processing. The injected particles are usually treated as a dispersed phase, governed by the equation of motion and the rate equations for heat and mass transfer in Lagrangian coordinates. A stochastic approach is introduced to take particle dispersion into account due to turbulent fluctuations by randomly sampling instantaneous flow fields. Three-dimensional effects are also considered which are mainly due to particle injection and the presence of a swirl component. A modified approach for investigating noncontinuum effects on plasma-particle heat transfer is proposed, incorporating both electric and aerodynamic effects on the boundary layer around a particle immersed into a thermal plasma. Comparisons of theoretical predictions based on the present model with available experimental data are, in general, in reasonable agreement.

KEY WORDS: Thermal plasma flows; particulates; three-dimensional effects; swirl component; modeling.

1. INTRODUCTION

The processing of fine particles, in the size range from submicron to hundred microns, represents one of the most important areas in thermal plasma processing. Some applications in thermal plasma processing today require injection of fine, solid particles into a plasma making use of the high energy and momentum content of such plasmas. Plasma-particle interaction manifests itself by thermal coupling through heat transfer, momentum coupling through aerodynamic drag, and mass coupling through evaporation.

A thermal plasma reactor is a highly heterogeneous system associated with steep temperature and velocity gradients. In spite of the high temperatures typical for thermal plasmas, such plasmas are not necessarily efficient heat sources for gas-solid reactions. This is due to the fact that a large number of injected particles may bypass the hottest zone, resulting in

[1] Department of Mechanical Engineering, University of Minnesota, Minneapolis, Minnesota 55455.

0272-4324/89/0300-0045$06.00/0

a relatively poor heat transfer to these particles. In many cases, only a small percentage of the energy supplied to the plasma torch is actually transferred to the particulate material being processed.

For some applications, it is also desirable that the particles acquire the proper amount of momentum from the plasma before impinging on a target (plasma spraying). One of the key factors for satisfying these requirements is the control of the trajectories and temperature histories of the particles, so that all particles receive adequate exposure to the hot plasma.

A theoretical investigation of thermal plasma systems, including plasma interaction with particulate matter, has been conducted in a recent thesis.[1] The behavior of plasma jets with superimposed vortex flow has been reported in an earlier paper.[2] The work described in this paper is concerned with the particle behavior in a thermal plasma flow, in particular with the influence of a turbulent plasma with superimposed vortex flow on particle behavior. This study should provide a better understanding of three important aspects of plasma processing: particle dynamics and heat and mass transfer. An attempt is made to improve the capability of existing modeling techniques and to point out major topics which need further research efforts. Realistic modeling of the interaction between plasmas and particulate matter is of great importance for industrial developments.

Gas-particle flows are found in many industrial applications, including combustion systems, cyclone separators and classifiers, fire safety systems, etc. Extensive investigations have been reported in the past years in these areas. Recent theoretical and experimental advances have created a renewed interest in the development of models for thermal spray processes. A literature survey of gas-particle flows in combustion systems has been provided in Ref. 1 and will not be included here.

In the following, earlier studies of gas-particle interaction in plasma systems will be briefly discussed, followed by an analysis of the present state-of-the-art for investigating particle behavior. The influence of injected particles on the gas flow will also be discussed.

2. BACKGROUND

Particles injected into a thermal plasma will encounter a highly heterogeneous environment with steep temperature and velocity gradients. Besides heat and momentum transfer between particles and the surrounding plasma, mass transfer due to particle vaporization, chemical reactions, or both may come into play under certain circumstances. These three transport processes interlink with each other and usually cannot be easily separated.

In principle, the models for gas-particle flows in ordinary fluids and in combustion systems can be adopted here. In addition, a number of effects which are insignificant or not present in ordinary gases will be experienced by particles immersed into a thermal plasma. Particle behavior in thermal plasmas has been reviewed in the early seventies,[3] and later reviews and papers of various aspects of generation and behavior of fine particles in thermal plasmas included detailed analyses of different terms involved in the equation of motion, and rate equations for heat and mass transfer.[4-6]

An understanding of the motion of particles within and around a plasma is essential for a detailed interpretation of the results of processing studies, as well as for heat and mass transfer between plasmas and particles. The basic forces acting on a particle injected into a thermal plasma are viscous drag and inertia. However, a number of additional effects might come into play in nonisothermal, heterogeneous flow systems such as thermal plasmas.

A few investigations based on a trajectory model have been reported in the literature[7-11] with emphasis on the analysis of particle dynamics including drag forces, Basset history terms, nonsphericity factors, thermophoresis, evaporation, and noncontinuum effects.

In the case of particle heating in plasmas, the main surface heat transfer mechanism has usually been taken to be conduction with or without convection. The most uncertain part for plasma-particle heat transfer (and also for mass transfer) is the proper correlation for the heat transfer coefficients or the Nusselt numbers (Nu). Due to large temperature gradients across the boundary layer and due to the highly nonlinear plasma properties, the conventional correlations derived from constant property flows must be corrected by variable property effects. A large variety of correction factors have been proposed over the past years. Comparisons among these proposals and comparisons with computer simulations and available experimental data have been reported.[6,12] Large discrepancies existing among various approaches for calculating heat transfer coefficients suggest that more work is necessary in the future to provide reliable data and correlations.

A number of effects encountered in plasma-particle heat transfer, including internal conduction, evaporation, unsteady heating, radiation, noncontinuum, and particle charging, are also reported in the literature.[6,13-19]

Whenever mass transfer occurs in thermal plasma processing, regardless of whether by evaporation or chemical reactions, heat transfer accompanies the entire exchange process. This implies that the mechanisms for heat and mass transfer are coupled.

Mass transfer from a particle surface heated by a thermal plasma may result from vapor diffusing across the liquid-vapor interface, driven by vapor concentration gradients existing between the free stream and the particle surface. Mass transfer can also occur as an intensive evaporation process from the particle surface when the surface temperature reaches or comes close to the boiling point of the particle material. Such heat and mass transfer studies between plasmas and particles have been reported over the past years.[6,14,20,21]

When the particle loading rate becomes relatively high compared to the plasma gas flow rate, the presence of the particles will affect the plasma fields. Then the plasma–particle interaction exerts a strong influence on both the particles as well as on the plasma. In addition, the presence of particle vapor, especially of some low-ionization-potential materials such as copper, must be included in the study of coupling effects.[22,23]

3. PARTICLE BEHAVIOR IN THERMAL PLASMAS

As described before, particles injected into a thermal plasma will experience a number of effects which are normally insignificant or not present in an ordinary fluid. Extensive studies of these effects and their relative importance have been reported in the past years. The emphasis in this paper is on improving the capability of the existing modeling techniques to make them more realistic for simulating plasma processes.

Three-dimensional effects, which are mainly due to particle injection and the presence of a swirl component, are included in the treatment of particle motions. A stochastic approach will be adopted to take particle dispersion into account due to turbulent fluctuations. In addition, the noncontinuum effect on heat transfer will be evaluated utilizing the concepts of plasma boundary layers and electrostatic probe theory. Mass transfer across the liquid–vapor interface has been investigated before[6] and will not be included here. Coupling effects are also excluded in this study due to the relatively low particle injection rate.

3.1. Particle Motion

The basic equation for the motion of a particle injected into a thermal plasma is established by a force balance. The inertia force of the injected particle is balanced by a viscous drag force as well as by a number of additional forces, namely, the pressure gradient force, the added mass term, the Bassett history term, external potential forces, and thermophoresis. The relative importance of these additional forces under different conditions of plasma systems have been investigated in the past. Details of the analyses may be found in the literature.[3,5,7–9]

Data considered in this work are mainly for alumina particles in the size range from 5 to 25 μm injected into a free plasma jet. Based on previous results the force balance for the equation of motion will be restricted to the viscous drag and inertia.

3.1.1. Equation of Motion

The equation of motion of a particle may be expressed in Lagrangian form as

$$\mathbf{F}=m_{\mathrm{p}}\frac{d\mathbf{v}_{\mathrm{p}}}{dt}=C_{\mathrm{D}}\frac{\pi d_{p}^{2}}{4}\frac{1}{2}\rho_{\mathrm{g}}|\mathbf{v}_{\mathrm{g}}-\mathbf{v}_{\mathrm{p}}|(\mathbf{v}_{\mathrm{g}}-\mathbf{v}_{\mathrm{p}}) \tag{1}$$

where the subscripts g and p represent local properties of the gas and particle, respectively. If this equation can be used in Cartesian coordinates, the difficulties with centrifugal and Coriolis accelerations at small radii can be avoided.(24) If cylindrical coordinates are used for the calculation of particle trajectories, the centrifugal and Coriolis forces have to be included in the governing equations.(25)

Integration of these equations provides the velocity components of the particles, from which the trajectories may be obtained by a further integration of the equation for the position vector $\mathbf{s}_{\mathrm{p}}$.

3.1.2. The Drag Coefficient

The drag force exerted on the particles can be deduced from a creeping flow situation, due to the small size (usually 5–100 μm in diameter) of particles used in thermal plasma processing. Different semiempirical relations for determining constant property drag coefficients on the film temperature exist in the literature, as for example

$$C_{\mathrm{Df}}=\frac{24}{\mathrm{Re}}+\frac{6}{1+\sqrt{\mathrm{Re}}}+0.4 \tag{2}$$

where the particle Reynolds number is based on the particle diameter and the relative velocity between the particle and the gas.

The temperature of a hot gas flowing over a sphere drops drastically in the boundary layer and, consequently, there are property variations across the boundary layer. Due to the steep temperature gradients between the particles and their surroundings as well as the highly nonlinear plasma properties, additional correction factors are needed for the drag coefficients. The correction factors proposed in Ref. 5 are adopted here, i.e.,

$$f_1=(\rho_{\infty}\mu_{\infty}/\rho_{\mathrm{w}}\mu_{\mathrm{w}})^{-0.45} \tag{3}$$

where the subscripts ∞ and w represent properties at the free stream and particle surface temperature, respectively.

Another correction factor should take the noncontinuum effects into account, which might be important due to the small particles used in thermal plasma processing:

$$f_2 = \left[1 + \left(\frac{2-a}{a}\right)\left(\frac{\gamma}{1+\gamma}\right)\frac{4}{\mathrm{Pr_w}}\,\mathrm{Kn}^*\right]^{-0.45} \tag{4}$$

where a is the thermal accommodation coefficient, γ the specific heat ratio, $\mathrm{Pr_w}$ the Prandtl number of the gas at the surface temperature of the particle, and Kn^* the Knudsen number based on an effective mean free path length.

Combining the above correction factors, we obtain a general expression for the drag coefficient, i.e.,

$$C_D = C_{Df} \cdot f_1 \cdot f_2 \tag{5}$$

3.1.3. Turbulent Dispersion of Particles

The nature of turbulent flows such as experienced in plasma spraying manifests itself by fluctuations and unsteadiness. The trajectories of particles injected into a fluctuating flow field will be dispersed due to the interactions with a series of turbulent eddies. A potentially useful stochastic approach has been proposed for gas–particle flows to account for the turbulence effects on droplet motion,[25] which has been evaluated later by a number of investigators.[24,26] This approach has been adopted for plasma–particle flows in Ref. 5.

The present model follows the existing one[5] closely, but it is extended to a three-dimensional situation in which the local plasma velocity fields are modified by including a randomly oriented fluctuation determined from two random numbers.

3.2. Particle Heating

When a particle is injected into a thermal plasma, it will experience large variations of the surrounding plasma temperature and velocity fields. This dramatically changing environment requires modifications of the conventional basic equations. A number of important effects have to be considered for plasma–particle heat transfer, including heat transfer associated with strongly varying plasma properties, unsteady heating, internal conduction, radiation, evaporation, noncontinuum conditions, etc. Extensive investigations have been undertaken over the past years.[11,13,16–18]. Results of these studies are summarized and discussed in Ref. 6.

3.2.1. Heat Transfer Equations

When a spherical particle enters a plasma flow, it is heated by the plasma. Heat flux to the particle from the plasma is dependent on the temperature difference between gas and particle surface and the heat transfer coefficient, which includes heat transfer by convection, radiation, and mass convection. The temperature history of the particle is determined by an energy balance at the particle surface, which includes the energy transfer from the plasma to the particle, the energy required for heating the particle to a certain temperature, the energy required for heating the vapor from the particle surface temperature to the plasma temperature, and the latent heat for phase change. In the case of melting or vaporizing, a moving-boundary problem must be solved.

The governing differential equation for the temperature distribution in a spherical particle is given by

$$\rho_p C_{p_p} \frac{\partial T}{\partial t} = \frac{1}{r^2} \frac{\partial}{\partial r}\left(\kappa_p r^2 \frac{\partial T}{\partial r}\right) \tag{6}$$

This type of equation can be solved by numerical methods with specified initial and boundary conditions. The initial particle temperature is assumed to be the same as the carrier gas temperature, which provides the necessary initial condition. A symmetry condition is applied in the center of the particle as one of the boundary conditions. The remaining boundary conditions for the particle depend on its state and have been described in detail in the literature.[6,14,15]

3.2.2. Convective Heat Transfer Coefficients

The convective heat transfer coefficients are usually evaluated from the transport properties taken at the film temperature using semiempirical correlations obtained experimentally. In the presence of moderate temperature gradients in a boundary layer, the heat transfer coefficient is obtained from a familiar Nusselt number correlation (Ranz-Marshall correlation),

$$\mathrm{Nu_f} = \frac{h d_p}{k_p} = 2.0 + 0.6\mathrm{Re}^{1/2}\mathrm{Pr}^{1/3} \tag{7}$$

A number of corrections are needed to make this correlation compatible with the plasma environment. The most important effect is due to the variable properties of the surrounding plasma, because of the large temperature gradients across the boundary layer. Another important factor is the noncontinuum effect, which will be discussed later.

Similar to the situation concerning the drag coefficient discussed before, a correction factor is required to account for the strongly varying properties in the boundary layer. A number of correction factors have been proposed in the past, and comprehensive evaluations have been published.[6,12] Unfortunately, large discrepancies exist among the proposed approaches for calculating heat transfer coefficients. This finding indicates the need for further studies, especially for particle heat and mass transfer under various plasma conditions, in order to develop reliable relationships. The correlation used in Ref. 6 will be adopted here.

$$\mathrm{Nu_f} = (2 + 0.6\mathrm{Re_f}^{1/2}\mathrm{Pr_f}^{1/3})\left(\frac{\rho_\infty \mu_\infty}{\rho_w \mu_w}\right)^{0.6}\left(\frac{C_{p_\infty}}{C_{p_w}}\right)^{0.38} \tag{8}$$

3.2.3. *Noncontinuum Effects*

The Knudsen effect (noncontinuum effect) on heat transfer to a particle exposed to a thermal plasma is important for many practical situations experienced in plasma chemistry and plasma processing. A "heat conduction potential jump" approach has been proposed to account for the Knudsen effect in these regimes.[18]. Further investigations showed that the ratio of the heat flux with and without Knudsen effect is almost the same for the case with and without convection.[19]

This approach was later modified by considering individual contributions to heat transfer from different species in a plasma, utilizing a limiting sphere concept and introducing the particle charging effect.[6] It is assumed that free molecular transport prevails within a limiting spherical shell while continuum transport is valid outside this shell. However, there are several key points which need further investigation, namely, the potential at the particle surface, the charged species density distribution across the shell, the heat transfer mechanisms for different species at the particle surface, etc.

In this paper, further investigation of the Knudsen effect is pursued, utilizing the concepts of electrostatic probe theory and plasma boundary layer theory as described for reentry studies. An attempt is made to modify the aforementioned approaches from a somewhat different point of view. A brief summary will be presented in the following, while details may be found in Ref. 1.

A particle injected into a thermal plasma is usually considered to be negatively charged due to the different thermal velocities and mobilities of electrons and ions. A comprehensive review concerning electric probes in stationary and flowing plasmas may be found in the literature.[27] An approach proposed in Ref. 28 will be adopted in the following for determining the surface potential of the negatively charged particle.

Definition of the sheath boundary conditions is a prerequisite for the analysis, since no true discontinuities occur in either the electric field or the charged particle density profiles. It is, therefore, postulated that the sheath is confined to the region in which the electric field becomes so large that all attracted particles entering the sheath are collected by the probe (cold solid surface).

The wall boundary conditions require consideration of the presence of the sheath. The continuum approach is used up to the edge of the assumed Knudsen layer, where the continuum and free molecular flow descriptions are matched. The total energy flux to the wall contains the contributions by heavy species, electrons, and recombination of ions and electrons, i.e.,

$$q_{\mathrm{T}} = q_{\mathrm{h}} + q_{\mathrm{e}} + q_{\mathrm{recom}} \tag{9}$$

For the heavy-species contribution, the convenient heat conduction potential concept may be applied. Then the heavy-species heat flux can be calculated from the following relation:

$$q_{\mathrm{h}} = -\kappa_{\mathrm{h}} \frac{dT}{dr} \frac{S_{\mathrm{h}\infty} = S_{\mathrm{hg}}}{r_{\mathrm{Kn}}} \tag{10}$$

where r_{Kn} is the radius of the Knudsen layer, $S_{\mathrm{h}\infty}$ and S_{hg} are the heavy-species heat conduction potential of the free stream and at r_{Kn}, respectively.

The continuity of the electron energy flux at the interface between the continuum and free molecular flow regime is applied to calculate the electron contribution at the edge of the Knudsen layer, i.e.,

$$q_{\mathrm{e}} = (2k_{\mathrm{B}}T_{\mathrm{e}} + |e\Phi|)n_{\mathrm{i}}c_{\mathrm{i}}/4 \tag{11}$$

where

$$c_{\mathrm{i}} = 4(k_{\mathrm{B}}T_{\mathrm{e}}/m_{\mathrm{i}})^{1/2} \tag{12}$$

The recombination of ions and electrons at the particle surface will release the recombination energy to the particle. Then

$$q_{\mathrm{recom}} = n_{\mathrm{i}}c_{\mathrm{i}}eE_{\mathrm{I}}/4 \tag{13}$$

where E_{i} is ionization potential.

It is assumed that the total heat flux at the edge of the Knudsen layer reaches the particle surface since this layer is so thin compared to the boundary layer thickness. Hence, the heat transfer to the particle from the plasma can be determined once the total heat flux at r_{Kn} is evaluated, which also provides the desired information of the Knudsen effect on heat transfer to small particles.

4. THEORETICAL PREDICTIONS

The model described in the previous sections is used to simulate particle behavior in a turbulent free plasma jet with superimposed vortex flow.

Alumina (Al_2O_3) particles in a size range from 5 to 25 μm are used in the experiment. Operating conditions for the plasma torch are the same as those described before. The plasma flow fields calculated in a previous paper[2] are used as the environment for the processing of particles. Due to the single port injection and the presence of the swirl component, particles injected into the plasma jet will follow a three-dimensional pattern, although the flow fields are considered to be two-dimensional (axisymmetric). The following considerations will focus on the effect of the swirl component on particle motion, and on the influence of the noncontinuum effect on plasma particle heat transfer.

4.1. Particle Motion in a Turbulent Plasma Jet with Superimposed Vortex Flow

A theoretical model[30] has been developed for comparing Laser Doppler anemometry (LDA) data[31] performed in the High Temperature Laboratory at the University of Minnesota with predictions. The previous model has been based on a two-dimensional approach with no swirl component and rotationally symmetric particle injection. The present model is based on a three-dimensional approach for particle motion, in order to account for the single-port injection and the effect of the swirl component.[32] This modification provides a significant contribution to the capability and flexibility of the model for simulating more complex plasma particle systems.

Cylindrical coordinates are used for the calculations, and the particle injector is placed at a location 5 mm downstream of the nozzle exit and 7 mm above the jet axis. The data recording system used in the LDA measurements has been based on Cartesian coordinates. Hence, a conversion from cylindrical to Cartesian coordinates is provided to link the results of simulations and measurements.

Figure 1 shows a qualitative sketch of particle trajectories without swirl component at different locations downstream of the nozzle exit. It can be seen that particles gradually penetrate into the axis of the plasma jet, preserving symmetry during lateral dispersion. Another side view of the envelope of the particle trajectories is plotted in Fig. 2. The trajectory of maximum particle number density is also given in the plot, which shows that the dispersion of the particles is not symmetric in the radial direction; the dispersion toward the jet axis is smaller than that toward the jet fringes. This phenomenon is due to the higher mean velocity and lower turbulent intensity in the center of a plasma jet, which reduces the relative importance of turbulent fluctuations in the center compared to the jet fringes.

A calculation of particle trajectories including all three velocity components (axial, radial, and tangential) is shown in Fig. 3. A right-hand or

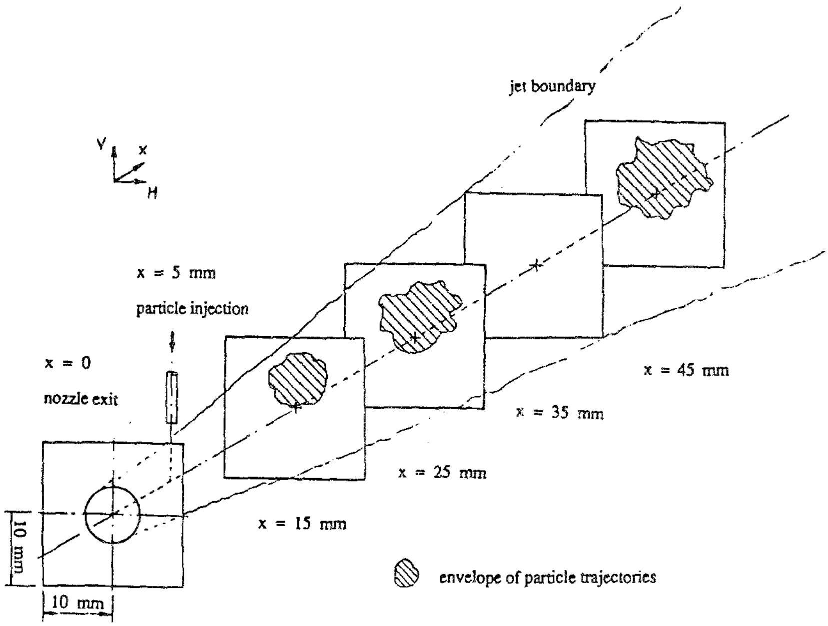

Fig. 1. Pattern of particle trajectories without swirl component.

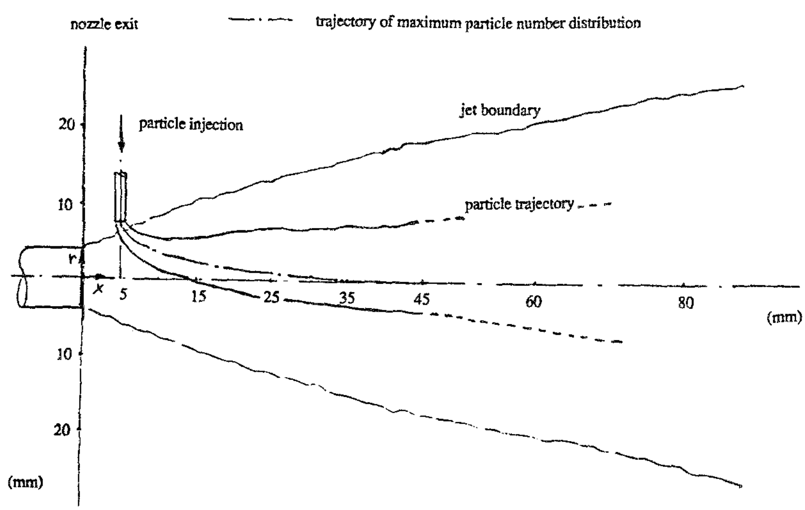

Fig. 2. Side view of particle trajectory pattern.

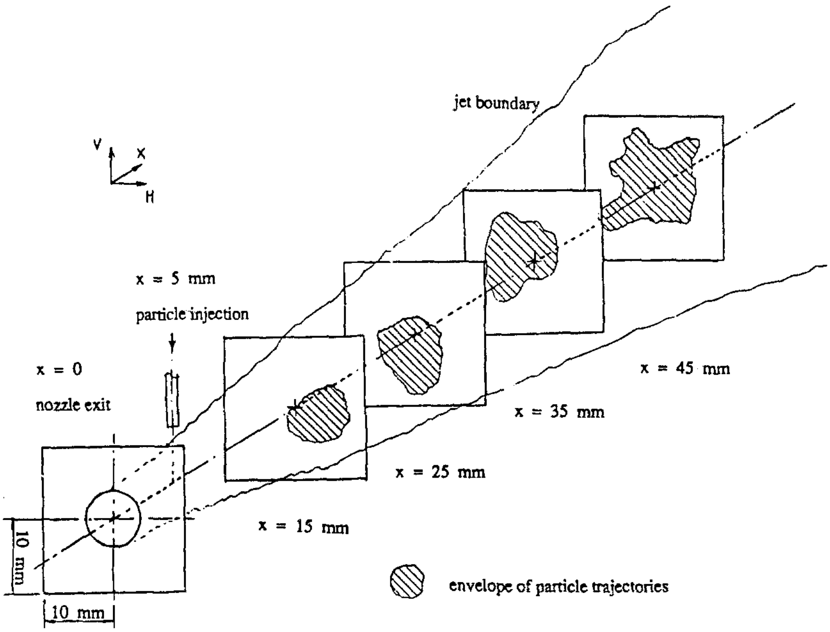

Fig. 3. Pattern of particle trajectories with right-handed swirl.

clockwise swirl component in the downstream direction is present in the flow field of the plasma jet. It is seen that particle motion is affected by the swirl component, leading to clockwise helical trajectories of the particles heading downstream with the plasma jet. However, the envelope of particle trajectories gradually becomes symmetric with respect to the jet axis, which means that the effect of the swirl component on particle motion diminishes farther downstream. This phenomenon is probably due to the fact that the swirl component diminishes rapidly downstream of the nozzle exit in a free jet.

4.2. Noncontinuum Effects on Heat Transfer

The importance of the noncontinuum effect during plasma processing of fine particles is a well-established fact. However, a comprehensive understanding of this phenomenon is still lacking. Refinement of existing models must rely on the availability of reliable experimental data for calibration, because there are a number of uncertainties involved in the theoretical derivations.

A simplifying assumption employed previously[6,18] is also used in the present work. It is assumed that a Knudsen layer or a limiting spherical shell exists around a particle in a thermal plasma. Free molecular transport is assumed within this shell, while continuum transport prevails outside this shell. Continuity of temperature and of heat flux corresponding to these regimes is matched at the edge of the shell.

A heat conduction potential jump distance has been introduced based on the temperature jump approach used in rarefied gas dynamics.[18] This jump distance has been placed at the edge of the Knudsen layer, which usually comprises several mean free path lengths, especially for small-diameter particles. This might not be appropriate since free molecular flow is assumed inside the Knudsen layer. Another uncertainty involved is the implication of LTE throughout the investigation domain, regardless of the existence of free molecular flow or continuum regimes. This assumption is questionable for plasma flows.

A modification was later proposed[6] by considering individual contributions to heat transfer from neutral species, ions, electrons, and recombination of ions and electrons. However, as mentioned before, this approach suffered from uncertainties such as the potential at the particle surface, the charged species density distributions across the shell, the heat transfer mechanisms for different species at the particle surface, etc.

The modification proposed in this paper is based on a boundary layer around a particle injected into a thermal plasma. This boundary layer incorporates both electrical and aerodynamic effects and can be divided into two subregions: an electric sheath, a characteristic phenomenon of plasma-wall interaction which may be regarded as an electrical boundary layer overlying the particle surface; and an aerodynamic boundary layer

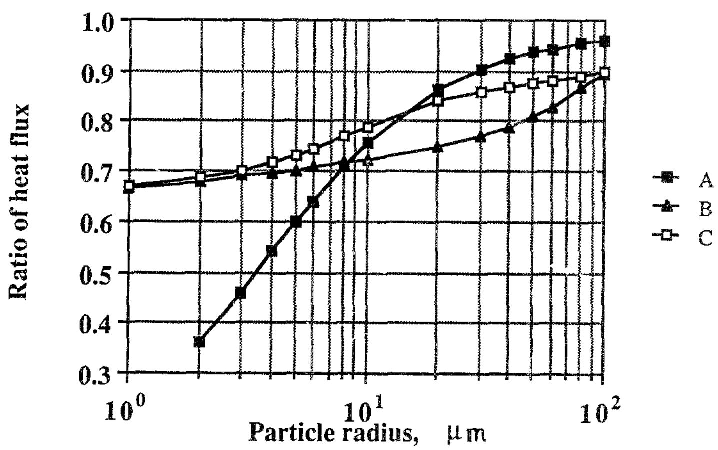

Fig. 4. Ratio of heat transfer with and without Knudsen effect; argon plasma ($T = 15{,}000$ K, particle surface temperature $T = 2500$ K). (A) Ref. 18; (B) Ref. 6; (C) present approach.

for momentum, thermal, and concentration transport outside the sheath and extending to the free-stream plasma. The edge of the Knudsen layer is chosen to be on the order of one man free path length to fulfill the prior assumption that free molecular flow prevails within this layer.

An illustrative result for this modification compared to previous investigations is shown in Fig. 4. The present result lies between the two curves derived from previous analyses in the temperature jump regime (for particle diameters greater than 10 μm), and approaches the curve based on the modified calculation[6] in the transition regime, which corresponds to a higher Knudsen number or a smaller particle diameter.

The present analysis includes both electrical and aerodynamic effects, which implies incorporation of the characteristic nature of plasma-wall interaction, and eliminates the uncertainties encountered in the previous work. This result provides a possible linkage between two different aspects of plasma physical processes: the electrical aspect, developed mainly in conjunction with electrostatic probe theory, and the continuum fluid mechanics approach for plasma flows. However, a comprehensive theory for plasma-particle systems is still in its infancy and more investigations, both theoretical and experimental, are necessary in the future.

5. CASE STUDIES

5.1. Particle Velocity in a Thermal Plasma Jet

A stochastic model for simulating particle behavior in plasma flows has been established in Section 3. This model will be used to calculate particle velocities in a plasma jet, and the computed results will be compared with experimental data from LDA measurements performed in the High Temperature Laboratory.[31]

As mentioned before, particles injected into a plasma flow will experience a heterogeneous environment with high temperature and velocity gradients. Thus, momentum and heat transfer between particles and the plasma vary from location to location. Particle trajectories and temperature histories are calculated in order to determine particle velocities and temperatures in flight. Theoretical considerations have been discussed before, and the computed results will be presented in the following.

The validity of the stochastic model depends greatly on full information on the initial injection conditions, including particle size and injection velocity distributions. Unfortunately, this information is not available for the data reported earlier, due to the difficulty imposed on experimental conditions. For example, the particle size distribution depends on the size range of the particles supplied and the operating conditions of the powder feeder. The latter might vary during a particular run. Furthermore, the particle size range is somewhat ambiguous due to the irregularity of particle shapes. Commercially supplied particles are usually irregular in shape, unless special precautions (e.g., spheroidization) are taken. It is also found that the particle diameters may not be limited to the size range specified by the supplier, because of large aspect ratios.

Due to the aforementioned incomplete information the experimental conditions, the comparison between the theoretical predictions and experimental data presented below will be less than perfect. The goal of this comparison is rather to search for the key parameters involved in the process and to provide guidance for future experimental work.

5.2. The Effect of the Gas Flow Field on the Particle Velocity

One of the important findings reported in Ref. 31 from LDA measurements of particle velocities in the plasma jet is that the particle acceleration within the plasma flow is not uniform along the axis. In most of the cases studied, particles are accelerated during the early stages after injection into the plasma, but gradually become decelerated further downstream, while calculations from an earlier model[30] predict continuous acceleration along the axis.

It should be noted that the previous model does not take into account any swirl component in the calculation of plasma fields. However, there is a strong swirl component according to the present torch design, which has strong effects on the plasma flow field. Hence, it is not surprising that inconsistencies exist between the present experimental data and the prediction from the previous model.

It has been speculated that the deceleration of particles further downstream in the plasma jet is due mainly to the plasma flow field. The axial velocity is reduced by the effect of the swirl component as compared to a situation without swirl. An investigation has been conducted to verify the suspected effect. The plasma temperature and flow fields have been computed from the modified parabolic model described in Ref. 2 with a swirl number of 0.32. In addition to the standard k–ε turbulence model, two modifications accounting for the streamline curvature effect on turbulence have also been incorporated in the calculation procedure. These modifications[33,34] are described in Ref. 1.

Particle behavior in the plasma flow was then simulated once the plasma fields were obtained. Particle velocities were calculated by an earlier two-dimensional model for simplicity, assuming annular injection of particles into the plasma. Injected particles were alumina in a size range from 5 to 25 μm. Spherical shape of the particles was also assumed for this illustration.

Figures 5–7 show the calculated results for different conditions as compared to the LDA measurements. An important phenomenon is observed from these results. The computed velocities for the case of a nonswirling jet, i.e., $S = 0$, show a monotonic acceleration in the axial direction as reported before, while the results for the case of $S = 0.32$ show

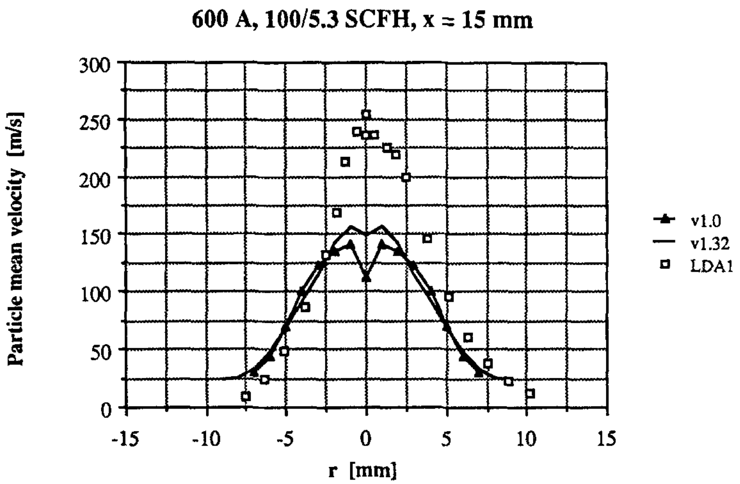

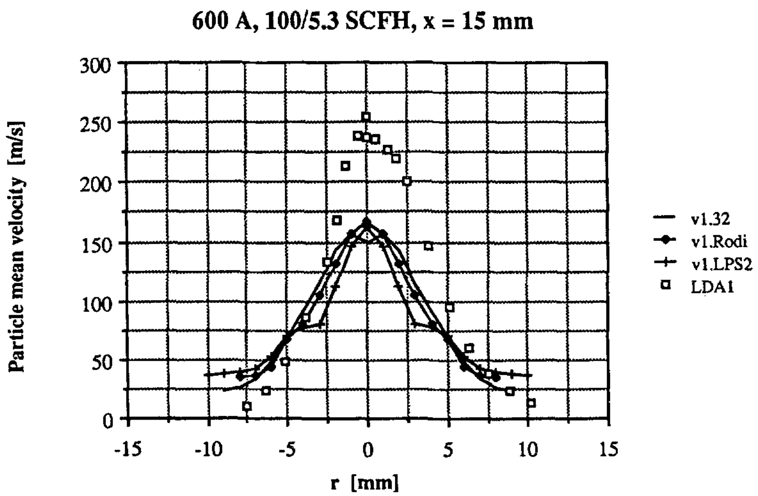

Fig. 5. Comparison of axial particle velocities; argon plasma jet, $I = 600$ A, $m = 1.4/0.07$ g/s (100/5.3 scfh). $x = 15$ mm; v1.0: Swirl number $S = 0$; v1.32: Swirl number $S = 0.32$; v1. Rodi: Ref. 34; v1. LPS2: Ref. 33; LDA1: experimental data.

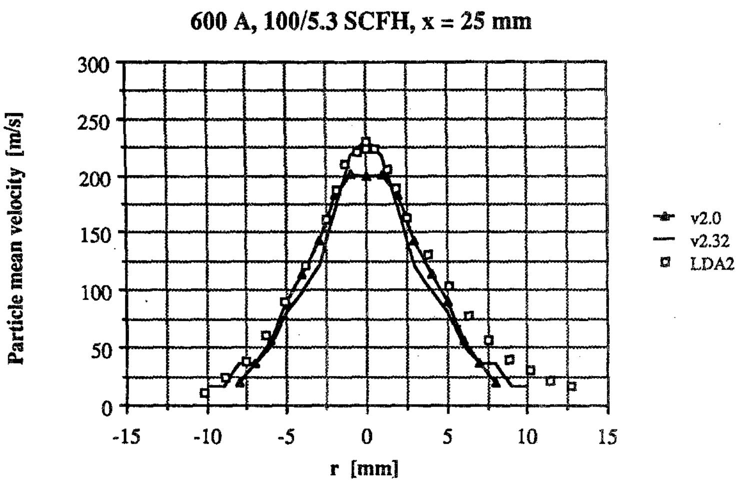

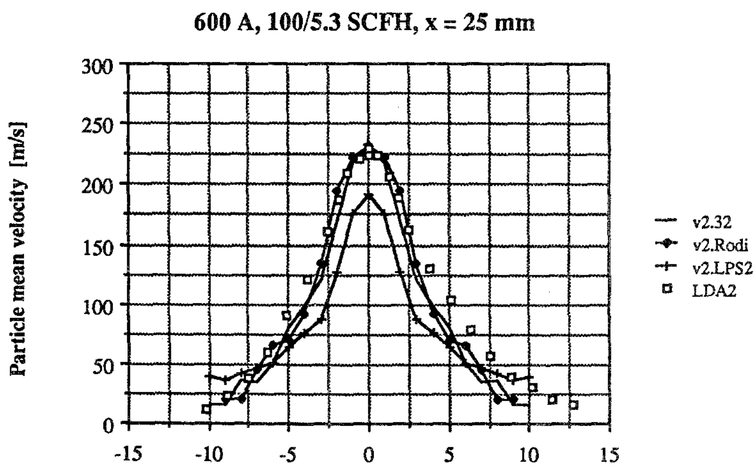

Fig. 6. Comparison of axial particle velocities; argon plasma jet, $I = 600$ A, $m = 1.4/0.07$ g/s (100/5.3 scfh). $x = 25$ mm; v2.0: Swirl number $S = 0$; v2.32: Swirl number $S = 0.32$; v2. Rodi: Ref. 34; v2. LPS: Ref. 33; LDA2: experimental data.

a different trend: acceleration in the upstream region and deceleration further downstream. These comparisons prove that the speculation mentioned earlier in this section is valid.

The LPS(33) and Rodi's(34) modifications for the streamline curvature effect on turbulence show somewhat different flow fields and, accordingly,

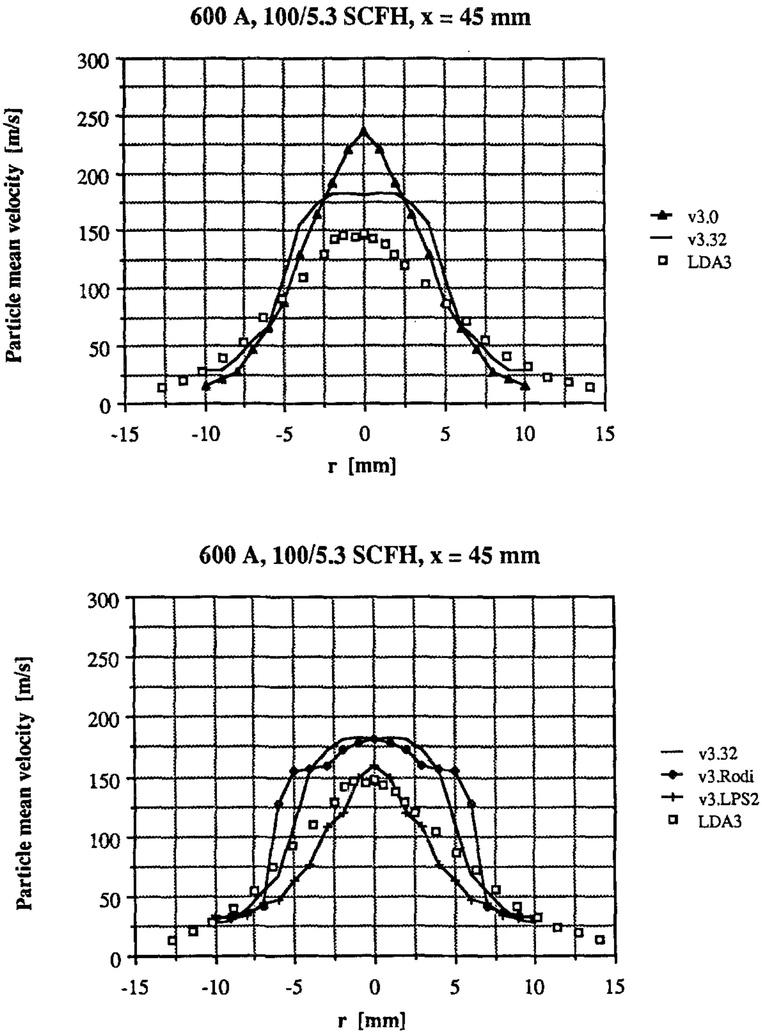

Fig. 7. Comparison of axial particle velocities; argon plasma jet, $I = 600$ A, $m = 1.4/0.07$ g/s (100/5.3 scfh). $x = 45$ mm; v3.0: Swirl number $S = 0$; v3.32: Swirl number $S = 0.32$; v3. Rodi: Ref. 34; v3.LPS: Ref. 33; LDA3: Experimental data.

particle velocities. But their validities have not yet been well tested, and no final conclusions can be drawn from these preliminary investigations.

It is also seen that the predictions agree fairly well with the experimental data at a location 25 mm downstream from the nozzle exit, while there is an underprediction at $x = 15$ mm, but an overprediction at $x = 45$ mm. The former might be due to the irregular shapes of the particles and the latter to the deflection of the jet axis by the injection. Both phenomena will be further discussed later in this section.

5.3. The Effect of Particle Shape on Particle Velocity and Drag Coefficient

Most of the particles injected into a plasma jet are originally irregularly shaped. Particle shapes, however, are changing during flight because of phase changes or deformation during the liquid phase. There is no rigorous study regarding particle shapes involved in thermal plasma processing. An example discussed in Ref. 8 includes shape effects on particle motion by treating a molybdenum disulfide powder as a thin disk, and as a sphere of equal volume when it reaches the melting point. But this consideration covers only a small part of possible shape effects.

A commonly cited terminology for measuring the shape of a particle is the *sphericity*, which is defined as the ratio of surface area of a sphere having the same volume to the actual surface area of the particle. The shape of a particle and its drag coefficient can be correlated by its sphericity and the Reynolds number, a correlation which can be found in the literature.[(35)] It is seen that the drag coefficient increases with decreasing particle Reynolds number of sphericity. For the same Reynolds number, the drag coefficients may vary by several orders of magnitude, corresponding to different shapes according to the correlation.

However, determination of the distribution of sphericity of commercial powders poses another difficulty in the experiment. Hence, the above correlation has no immediate usefulness at present. The shape effect on particle velocities is believed to have a more pronounced influence at the early stages of the particle trajectories than during the later part. This is due to the fact that particles will be heated up during flight, and the assumption of spherical particles would be reasonable after they reach the melting point. Thus, it is not surprising that the predictions from models which assume spherical particles underestimate particle velocities at the early stages of the particle trajectories as, for example, at the location $x = 15$ mm.

In order to investigate the effect of particle shape on the drag coefficient (or particle velocity), a simple test run has been performed. Based on a spherical particle assumption, the drag coefficient has been increased by a factor of 3 and 5 in excess of the values obtained from the correlation (only for computational purposes), and the calculated results are shown in Fig. 8. The particle velocity increases with increasing drag coefficient, and the curve with $5C_D$ seems to be in reasonable agreement with the experimental data at $x = 15$ mm. This comparison demonstrates that the particle shape

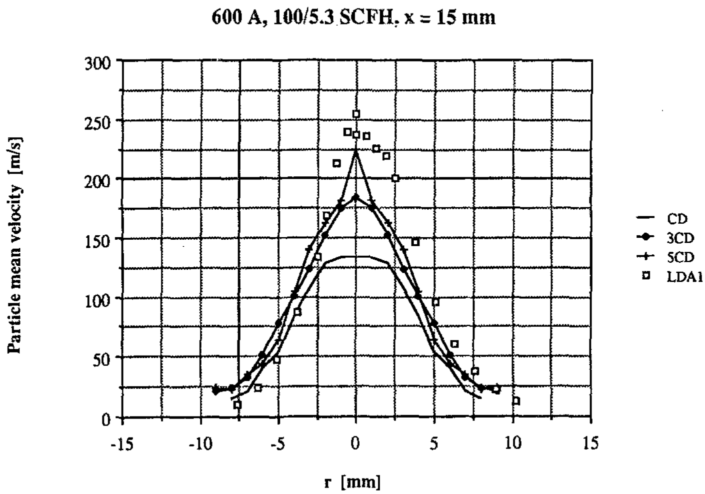

Fig. 8. Effect of the drag coefficient on the particle velocity; argon plasma jet, $I = 600\ A$, $\dot{m} = 1.4/0.07$ g/s (100/5.3 scfh). $x = 15$ mm; CD: drag coefficients for a spherical particle; 3CD: increased by a factor of 3; 5CD: increased by a factor of 5; LDA1: experimental data.

effect on the particle velocity is important, especially at the early stages of the particle trajectories. Any meaningful comparison between theoretical prediction and experimental data must be based on reliable information about particle shapes.

In order to circumvent this difficulty of determining the sphericity distribution of commercially supplied powders, it is recommended that the injected particles be pretreated before running experiments. Spheroidization seems to be a useful process to form particles with nearly spherical shapes.

5.4. The Deflection of the Jet due to Particle Injection

The present model considers three-dimensional motion of particles due to the single-port injection in the experimental set-up and the presence of the swirl component. The extension to three dimensions provides complete information on particle behavior at any location inside a plasma jet and a large degree of flexibility for adapting the model to different types of geometries used for experiments. This is essential for present as well as for future investigations. For example, the investigation of the deflection of the jet from the geometric axis can be easily incorporated into the model, since all the interesting information is recorded in a three-dimensional storage, covering all of the calculation domain.

It has been found that a plasma jet is deflected away from its geometrical axis due to particle injection perpendicular to the axis. The deflection angle of the plasma jet increases with increasing injection flow rate. This phenomenon is very important for the study of particle velocities in a plasma jet, because LDA measurements usually need injection of particles as tracers into the plasma jet studied. But the injection may deflect the jet, i.e., the jet axis may deviate from the geometrical axis. This deviation becomes even more pronounced further downstream. For example, in the present experimental set-up in the High Temperature Laboratory, the particle injector is located 5 mm downstream of the nozzle exit and three recording locations are placed further downstream at 15, 25, and 45 mm. Considering a deflection angle of 5°, the deviation of the jet axis from the geometrical axis at the first recording location ($x = 15$ mm) is around 0.87 mm, but increases to 1.75 mm at the second recording location ($x = 25$ mm) and even to 3.5 mm at $x = 45$ mm. These deviations may cause significant differences in the resulting particle velocities because of the steep velocity gradients characteristic for plasma flows.

Computations have been performed utilizing the three-dimensional model for particle velocities as described above. The same plasma fields used in the previous calculations have been applied. Results are presented for two downstream locations, at $x = 25$ mm and at $x = 45$ mm, in order to demonstrate the effect of jet deflection.

As a first step, dispersion of particle motion in the lateral direction due to turbulent fluctuations are considered by setting the mean tangential velocities to zero in order to eliminate the rotation of particle trajectories. This procedure is used mainly for easier identification of the locus of particle trajectories. Its effect on particle velocity will be discussed later. It is found that particle dispersion due to turbulence predicted by the model seems to have been underestimated as compared to experimental data. For example, particles can be found, according to the prediction, between a range from -8 mm to $+6$ mm in the horizontal direction at the location $x = 25$ mm. But the experimental data show a range from -10.2 mm to $+12.7$ mm at the same location.

Particle mean velocities are also evaluated by the same calculations and compared with the LDA measurements. Figure 9 shows the results at the 2nd recording station, $x = 25$ mm, in which Up2.cl represents the predicted values for an undeflected jet axis, Up2.3 denotes the predicted velocities at the axis with a 3° deflection, and LDA2 shows the experimental data. The same notations are used in Fig. 10 which shows the results at the 3rd recording station, $x = 45$ mm. The deviation of the jet axis with 3° deflection from the geometrical axis is around 1 mm at the 2nd recording station and about 2 mm at the 3rd recording station. As shown in Fig. 9,

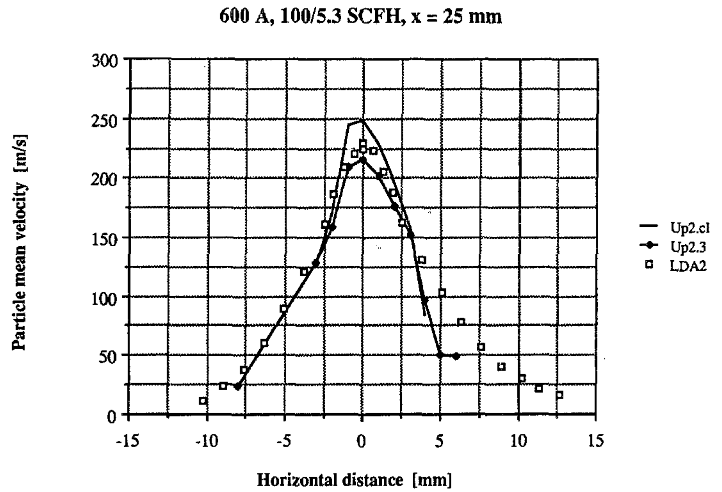

Fig. 9. Comparison of axial particle velocities; argon plasma jet, $I = 600$ A, $\dot{m} = 1.4/0.07$ g/s (100/5.3 scfh); $x = 25$ mm; Up2.cl: predicted values for nondeflected jet axis; Up2.3: predicted values for 3° deflection; LDA2: experimental data.

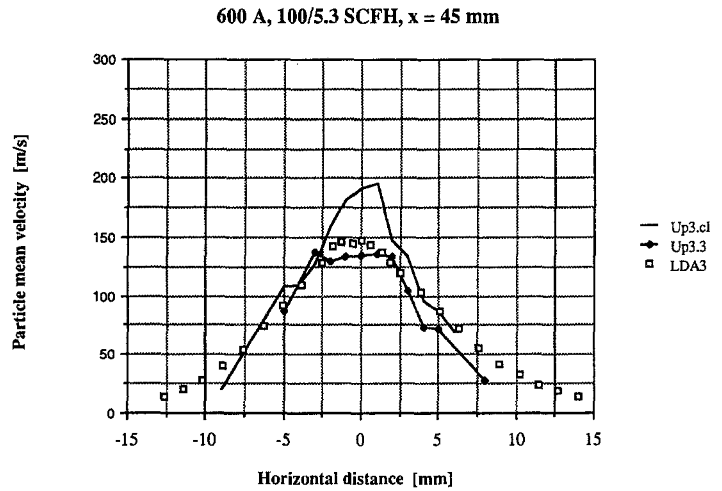

Fig. 10. Comparisons of axial particle velocities; argon plasma jet, $I = 600$ A, $\dot{m} = 1.4/0.07$ g/s (100/5.3 scfh). $x = 45$ mm; Up3.cl: predicted values for nondeflected jet axis; Up3.3: predicted values for 3° deflection; LDA3: experimental data.

600 A, 100/5.3 SCFH, X = 25 mm

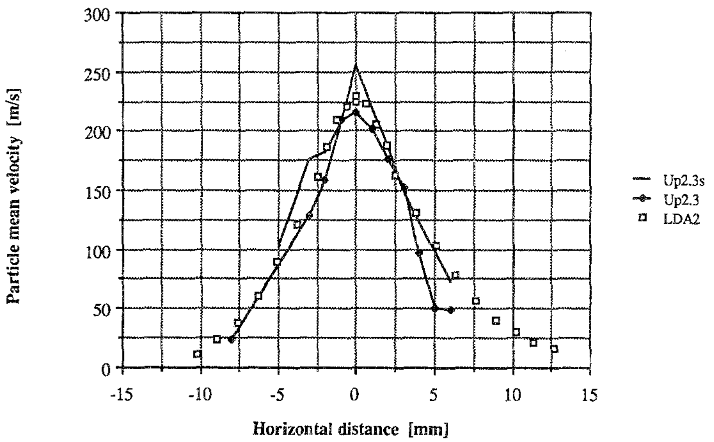

Fig. 11. Comparison of axial particle velocities; argon plasma jet, $I = 600$ A, $\dot{m} = 1.4/0.07$ g/s (100/5.3 scfh); $x = 25$ mm; Up2.3s: prediction according to this calculation; Up2.3: prediction without considering mean tangential velocity; LDA2: experimental data.

600 A, 100/5.3 SCFH, x = 45 mm

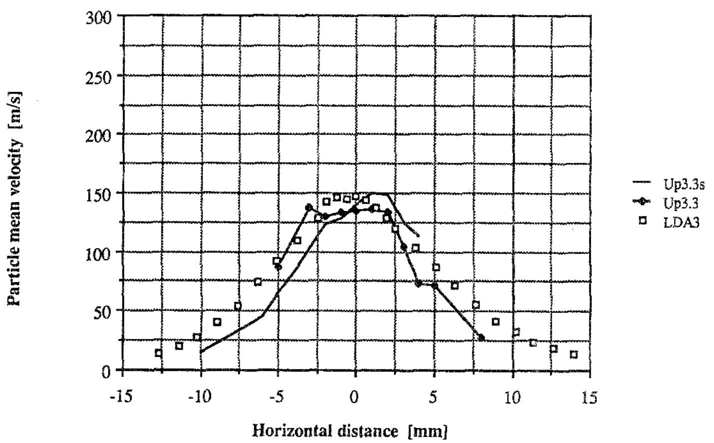

Fig. 12. Comparison of axial particle velocities; argon plasma jet, $I = 600$ A, $\dot{m} = 1.4/0.07$ g/s (100/5.3 scfh). $x = 45$ mm; Up3.3s: prediction according to this calculation; Up3.3: prediction without considering mean tangential velocity; LDA3: experimental data.

the centerline particle velocity drops from 248 to 216 m/s within 1 mm from the axis. As compared to the measured data, 229.7 and 224.2 m/s, the prediction assuming a small deflection angle of the jet gives a better agreement with the experimental data. This procedure is justified by the results shown in Fig. 10. The centerline particle velocity drops from 192 to 135 m/s within 2 mm from the axis, whereas the measured data indicate values of 146.9 and 148 m/s.

Further computations have been performed for a complete three-dimensional motion of particles, taking into account both mean and fluctuating parts of gas velocities in all three directions (axial, radial, and tangential). The results are also compared with the previous predictions and the experimental data. According to the previous discussion, the jet deflection angle is taken as 3°. Figure 11 shows the results at the 2nd recording station, $x = 25$ mm. The curve marked Up2.3s represents the prediction from the current calculation. It is somewhat different from the previous prediction Up2.3, which neglects the mean tangential velocity in the calculations, but both predictions, in general, fall in the right range of magnitude compared to the experimental data. The results at $x = 45$ mm are shown in Fig. 12, in which Up3.3s denotes the current prediction. Again, the overall agreement between both predictions and experimental data may be regarded as satisfactory.

5.5. Discussion

Encouraging agreement between theoretical predictions and experimental data for particle velocities in a turbulent thermal plasma jet with superimposed vortex flow have been obtained throughout these analyses. Due to the lack of information on particles and particle injection into the plasma jet, the aforementioned analyses are not focused on achieving perfect agreement with measurements, but rather on determining some important parameters involved in the process. Knowledge derived from the present comparisons should provide guidance for future work.

As mentioned in Section 3, the present stochastic model for simulating particle motion in plasma flows requires a statistically significant number of particles to adequately represent the ensemble-averaged mean quantities such as particle velocities, temperatures, etc. A few hundred particles were simulated in the present illustrations, but this number is still considerably lower than that required from a statistical point of view. Hence, there are some nonsmooth predictions for turbulent dispersion of particle motion. From a theoretical point of view, this underprediction may be due to the initial conditions of the injected particles (particle size and injection velocity distributions). Another possible reason may be the random sampling process for the turbulent velocity field. However, a closer look at the experimental data reveals that the standard deviations are comparable or even larger than the mean quantities at the outer fringes of the jet. The particle velocity distributions are wider on a relative base in this region as compared to the core of the jet. Uncertainties may exist for these distributions stemming either from real particle signals or from background noise.

The injection flow rate (5.3 scfh) is relatively small, about 5% of the main flow rate (100 scfh) for the case illustrated above. The deflection of the jet axis is believed to be minimal. However, it has been shown that even a very small deflection angle of 3° will cause a substantial difference of particle velocities further downstream. This finding is very important for a correct interpretation of experimental data, since LDA measurements always require injection of particles as tracers into the flow field and the operating conditions studied here are typical for this kind of experiment. Failure to take into account the possible deflection of the jet axis due to injection may result in erroneous interpretation of experimental data. In order to prevent incorrect interpretation of experimental data, it is recommended that future measurements be recorded at several radial locations rather than only on the geometrical axis. This would provide sufficient information for determining the effect of the deflection of the jet axis, avoiding incorrect conclusions in this way.

In summary, the present stochastic model for simulating three-dimensional particle motion in turbulent plasma jets with superimposed vortex flow has provided an important contribution to the understanding of particle behavior in thermal plasma flows. It serves as a useful tool for further investigation of thermal plasma processing. Further refinement should be pursued both in terms of theoretical modeling as well as in experimental work.

6. CONCLUSIONS

1. A three-dimensional stochastic model for simulating particle behavior in turbulent plasma jets with superimposed vortex flow shows that particle motion is strongly affected by the swirl component, especially in the vicinity of the injection port. The predictions of particle trajectories are qualitatively consistent with experimental observations.

2. A modified approach for investigating the Knudsen effect on plasma-particle heat transfer shows that the heat conduction jump approach overestimates the reduction of heat transfer for smaller particle sizes.

3. The theoretical model developed in this study reveals that a small deflection of the jet axis due to non-symmetric injection has an important effect on the interpretation of experimental data. Satisfactory agreement

between theory and experiment is achieved after taking the effect of the swirl flow into account and the deflection of the plasma jet axis.

ACKNOWLEDGMENT

This work has been supported by DOE/FG02-85ER-13433.

REFERENCES

1. Y. P. Chyou, "Modeling of Thermal Plasma Systems," Ph.D. Thesis, Department of Mechanical Engineering, University of Minnesota (1987).
2. Y. P. Chyou and E. Pfender, "Plasma Jets with Superimposed Vortex Flows" (1988), to be published.
3. B. Waldie, "Review of Recent Work on the Processing of Powders in High-Temperature Plasmas, Part II: Particle Dynamics, Heat Transfer, and Mass Transfer," *Chem. Eng.* (London), 188 (1972).
4. R. M. Young, and E. Pfender, "Generation and Behavior of Fine Particles in Thermal Plasmas—A Review," *Plasma Chem. Plasma Process.* **5**, 1 (1985).
5. E. Pfender and Y. C. Lee, "Particle Dynamics and Particle Heat and Mass Transfer in Thermal Plamas, Part I: The Motion of a Single Particle without Thermal Effects," *Plasma Chem. Plasma Process* **5**, 211 (1985).
6. Y. C. Lee, Y. P. Chyou, and E. Pfender, "Particle Dynamics and Particle Heat and Mass Transfer in Thermal Plasmas, Part II: Particle Heat and Mass Transfer in Thermal Plasmas," *Plasma Chem. Plasma Process.* **5**, 391 (1985).
7. J. A. Lewis and W. H. Gauvin, "Motion of Particles Entrained in a Plasma Jet," *AIChE J.*, **19**, 982 (1973).
8. M. I. Boulos and W. H. Gauvin, "Powder Processing in a Plasma Jet: A Proposed Model," *Can. J. Chem. Eng.* **52**, 355 (1974).
9. C. Sheer, S. Korman, D. J. Angier, and R. P. Cahn, "Arc Vaporization of Refractory Powders," in *Fine Particles*, Second Intern. Conf., W. E. Kuhn, ed. (1974), p. 133.
10. Y. C. Lee, K. C. Hsu, and E. Pfender, "Modeling of Particles Injected into a D.C. Plasma Jet," Proceedings of the 5th Intern. Symp. on Plasma Chem., B. Waldie and G. A. Farnell, eds., University of Edinburgh, Edinburgh, Scotland, Vol. 2 (1981), p. 795.
11. X. Chen, Y. C. Lee, and E. Pfender, "The Importance of Knudsen and Evaporation Effects on Modeling in Thermal Plasma Processing," Proc. of the 6th Intern. Symp. on Plasma Chemistry, M. I. Boulos and R. J. Munz, eds., McGill University, Montreal, Canada, Vol. 1 (1983), p. 51.
12. R. M. Young and E. Pfender, "Nusselt Number Correlations for Heat Transfer to Small Spheres in Thermal Plasma Flows," *Plasma Chem. Plasma Process.* **7**, 211 (1987).
13. E. Bourdin, P. Fauchais, and M. Boulos, "Transient Heat Conduction under Plasma Conditions," *Int. J. Heat Mass Transfer* **26**, 567 (1983).
14. T. Yoshida and K. Akashi, "Particle Heating in a Radio-Frequency Plasma Torch," *J. Appl. Phys.* **48**, 2252 (1977).
15. J. K. Fiszdon, "Melting of Powder Grains in a Plasma Flame," *Int. J. Heat and Mass Transfer* **22**, 749 (1979).
16. X. Chen and E. Pfender, "Heat Transfer to a Single Particle Exposed to a Thermal Plasma," *Plasma Chem. Plasma Processs* **2**, 185 (1982).
17. X. Chen and E. Pfender, "Unsteady Heating and Radiation Effects of Small Particles in a Thermal Plasma," *Plasma Chem. Plasma Process.* **2**, 293 (1982).

18. X. Chen and E. Pfender, "Effect of the Knudsen Number on Heat Transfer to a Particle Immersed into a Thermal Plasma," *Plasma Chem. Plasma Process.* **3**, 97 (1983).
19. X. Chen and E. Pfender, "Behavior of Small Particles in a Thermal Plasma Flow," *Plasma Chem Plasma Process.* **3**, 351 (1983).
20. F. J. Harvey and T. N. Meyer, "A Model of Liquid Metal Droplet Vaporization in Arc-Heated Gas Streams," *Metall. Trans. B* **9**, 615 (1978).
21. M. A. Luzhnova and Ya. D. Daikhbaum, "Kinetics of Metal Particle Vaporation in an Arc Plasma," *High Temp.* **7**, 283 (1969).
22. P. Proulx, J. Mostaghimi, and M. I. Boulos, "Plasma-particle Interaction Effects in Induction Plasma Modeling under Dense Loading Conditions," *Int. J. Heat Mass Transfer* **28**, 1327 (1985).
23. Y. P. Chyou, R. M. Young and E. Pfender, "The Effect of Particle Loading on the Behaviour of a High-Intensity Arc," Proc. of the 7th Intern. Symp. on Plasma Chem., C. J. Timmermans, ed., University of Eindhoven, Eindhoven, The Netherlands, Vol. 3 (1985), p. 892.
24. P. P. Chen and C. T. Crowe, "On the Monte Carlo Method for Modeling Particle Dispersion in Turbulence," in *Gas-Solid Flows*, ASMS FED., J. T. Jurewicz, ed., Energy Sources Technology Conference, New Orleans, Louisiana, Vol. 10 (1984).
25. A. D. Gosman and E. Ionnides, "Aspects of Computer Simulation of Liquid-Fuelled Combustors," AIAA Paper No. 81-0323, AIAA 19th Aerospace Science Meeting, St. Louis, Missouri (1981).
26. J. S. Shuen, L. D. Chen, and G. M. Faeth, "Evaluation of a Stochastic Model of Particle Dispersion in a Turbulent Round Jet," *AIChE J.*, **29**, 167 (1983).
27. P. M. Chung, L. Talbot, and K. J. Touryan, "Electric Probes in Stationary and Flowing Plasmas," 2 parts, *AIAA J.* **12**, 133 (1974).
28. R. E. Kiel, "Electrostatic Probe Theory for Free-Molecular Spheres," *AIAA J.* **9**, 1380 (1971).
29. M. Camac and N. H. Kemp, "A Multitemperature Boundary Layer," AIAA Paper No. 63-460, AVCO Everett Research Laboratory, Research Report 184, Contract No. NAS w-748 (1964).
30. Y. C. Lee, "Modeling Work in Thermal Plasma Processing," Ph.D. Thesis, Department of Mechanical Engineering, University of Minnesota (1984).
31. E. Fleck, "Temperature and Velocity Measurements of Thermal Plasma Jets," Ph.D. Thesis, Department of Mechanical Engineering, University of Minnesota (1986).
32. Y. P. Chyou and E. Pfender, "Studies of Gas-Particle Flows in Turbulent Swirling Plasma Jets," Proc. of the 8th Intern. Symp. on Plasma Chemistry, K. Akashi and A. Kinbara, eds., University of Tokyo, Tokyo, Japan, Vol. 1 (1987), p. 101.
33. B. E. Launder, C. H. Priddin, and B. I. Sharma, "The Calculation of Turbulent Boundary Layers on Spinning and Curved Surfaces," *Trans. ASME: J. Fluids Eng.* **99**, 231 (1977).
34. W. Rodi, "Influence of Buoyancy and Rotation on Equations for the Turbulent Length Scale," Proc. of the 2nd Symp. on Turbulent Shear Flows, Imperial College, London (1979), pp. 10.37-10.42.
35. G. E. Klinzing, *Gas-Solid Transport*, McGraw-Hill, New York (1981).